ISSN: 2538-2152; ECOPERSIA. 2018;6(4):241-257

Valuation of Object-Based and Decision Tree Classification Methods in Estimating the Quantitative Characteristics of Single Oak Trees on WorldView-2 and UAV Images

ARTICLE INFO

Article Type
Original Research

Authors
Taghi Mollaei Y.*[1] *PhD*,
Karamshahi A.[1] *PhD*,
Erfanifard S.Y.[2] *PhD*

How to cite this article
Taghi Mollaei Y, Karamshahi A, Erfanifard S Y. Valuation of Object-Based and Decision Tree Classification Methods in Estimating the Quantitative Characteristics of Single Oak Trees on WorldView-2 and UAV Images. ECOPERSIA. 2018;6(4):241-257.

[1]Forest Sciences Department, Agriculture & Natural Resources Faculty, Ilam University, Ilam, Iran
[2]Natural Resources & Environment Department, Agriculture Faculty, Shiraz University, Shiraz, Iran

***Correspondence**
Address: Forest Sciences Department, Pazhohesh Boulevard, Ilam Province, Iran
Phone: +98 (84) 32234850
Fax: +98 (84) 32227015
taghimollei@yahoo.com

Article History
Received: April 13, 2018
Accepted: September 02, 2018
ePublished: November 21, 2018

ABSTRACT

Aims One of the most commonly used applications in forestry is the identification of single trees and tree species compassions using object-based image analysis (OBIA) and classification of satellite or aerial images. The aims of this study were the valuation of OBIA and decision tree (DT) classification methods in estimating the quantitative characteristics of single oak trees on WorldView-2 and unmanned aerial vehicle (UAV) images.

Materials & Methods In this experimental study Haft-Barm forest, Shiraz, Iran, was considered as the study area in order to examine the potential of Worldview-2 satellite imagery. The estimation of forest parameters was evaluated by focusing on single tree extraction using OBIA and DT methods of classification with a complex matrix evaluation and area under operating characteristic curve (AUC) method with the help of the 4th UAV phantom bird image in two distinct regions. Data were analyzed by paired t-test, multivariate regression analysis, using SPSS 25, Excel 2016, eCognation v. 8.7, ENVI, 5, PCI Geomatica 16, and Google Earth 7.3 Software.

Findings The base object classification had the highest and best accuracy in estimating single-tree parameters. Basic object classification method was a very useful method for identifying Oak tree Zagros Mountains forest. With using WV-2 data, the parameters of single trees in the forest can extract.

Conclusion The accuracy of OBIA is 83%. While UAV has the potential to provide flexible and feasible solutions for forest mapping, some issues related to image quality still need to be addressed in order to improve the classification performance.

Keywords Separation of Single Trees; Canopy; Remote Sensing; Classification; Haft-Barm of Shiraz

CITATION LINKS

[1] Comparing ALS and Image-Based ... [2] Imputing forest structure attributes ... [3] Response of plants to multiple ... [4] Towards automated segmentation of ... [5] A global overview of drought and ... [6] Regional vegetation die-off in ... [7] Widespread crown condition ... [8] Drought sensitivity of the Amazon ... [9] Widespread increase of tree mortality ... [10] Tree crown mapping in managed ... [11] Quantifying mortality of tropical ... [12] Application of 1-M and 4-M resolution ... [13] Photo ecometrics for forest ... [14] Analysis of high spatial resolution ... [15] Airborne digital camera image ... [16] A comparison of standard ... [17] Classification of tree species ... [18] Comparing pixel and object-based ... [19] Comparison of support vector ... [20] Comparison of Pixel-Based ... [21] Extraction of individual ... [22] Determining the water ... [23] Radiometric use of ... [24] PHANTOM 4 user ... [25] Learning with continuous ... [26] Ecological study on the ... [27] An Object-Based classification ... [28] Extracting urban vegetation ... [29] Decision Tree Classification ... [30] Decision tree classification ... [31] An assessment of the effectiveness ... [32] Introductory digital image ... [33] Induction of decision ... [34] Decision tree regression for ... [35] Remote Sensing: Models ... [36] The factor of scale in ... [37] Multi-resolution, object-oriented ... [38] ESP: A tool to estimate scale ... [39] Automated parameterisation ... [40] Semantic classification of ... [41] Tree Species Classification ... [42] Object-based analysis ... [43] Forest change detection ... [44] An automated object-based ... [45] Object-Based ... [46] Identifying mangrove ... [47] Integration of object-based ... [48] Estimating biophysical ... [49] Object-based classification ... [50] Comparison of random ... [51] Comparing machine learning ... [52] A comparison of support ... [53] Comparison of support ... [54] Empirical comparison ... [55] Comparison of methods ... [56] Comparing image classification ... [57] Comparison of hybrid classifiers for ... [58] Unsupervised texture segmentation in ... [59] Texture segmentation using fractal ... [60] Multiresolution segmentation-an ... [61] Object-based image analysis ... [62] Multilevel object-oriented ... [63] Pixel-based and object-oriented ... [64] The improvement of an ... [65] Granular approach to object-oriented ... [66] An object-oriented approach to ... [67] Comparison of object-based ... [68] A medium-resolution remote ... [69] Assessment of forest tree structural ...

Introduction

Forest inventory is traditionally a useful and accurate way of monitoring forest coverage, but it is very expensive and its updating cycle is relatively expensive because of its cost [1-3]. Wide range of forest can undergo rapid changes; forest inventory traditionally does not respond adequately to the development of change [4]. Climate warming and recent severe droughts have resulted in vegetation mortality in various woody biomes across the globe [5-9].

The separation of single trees and the extraction of tree-related structural data from remote sensing data have a prominent application in a variety of activities. For example, detailed information on the level of individual trees can be used to monitor forest regeneration [10-12]. The reduction of fieldwork required for surveying [13] and damage assessment is used in the forest [14-16].

In previous studies, the accuracy of estimating the crown area is made, using field data, in which the shape of the crown of the trees is generally considered circular and the crown area is obtained from the mean diameter, provided that the trees, according to the possible vegetative conditions, it has crowns with non-hinged shapes. Therefore, it is necessary to assess the accuracy of crown areas estimated in satellite data, using more reliable data such as unmanned aerial vehicle (UAV) aerial imagery.

Remote sensing provides data types and useful resources for forest mapping. Today, one of the most commonly used applications in forestry is the identification of single trees and tree species compassions, using object-based analysis and classification of satellite or aerial images. Sedliak *et al.* [17] identified the groups of trees (Leaf-leaf needles) in individual structures of massive mixed grass, spruce, and pine forests in worldview-2 (WV-2) images. The object-based classification with WV-2 multispectral images as well as the data in the eCognation software was used. Lidar data allowed the identification of single trees and the overall high accuracy was 87.42%. The accuracy of the needle calves rose from 82.93 to 85.73% and broadband ranged from 84.79 to 90.16%.

Basic object classification method is a very useful method for identifying wild plants in numerous habitats. Niphadkar *et al.* [18] used WV-2 images to identify shrubs in the tropical forest. The base object method, with the help of spatial and spatial characteristics of the feature, is capable of separating the features, and the environment perfectly separates each object from the rest of the coating. As a result, with a non-parametric classification algorithm, we were able to isolate the shrub in a complex environment of tropical forests.

The accuracy of the tree species map allows us to carry out in-depth, more detailed analyzes of forest biophysical variables. Raczko and Zagajewski [19] compared the support vector algorithm, random forest and neural network for the tree species class on aerospace aerial imagery. The study showed that the artificial neural networks (ANN) classification had the highest classification accuracy (77%), and Support Vector Machines (SVM) with 68% and Random forest (RF) with 62% respectively in the next steps.

Juniati and Arrofiqoh [20] compared the base pixel and base object classification, using parametric and nonparametric methods for pattern matching in Indonesian forests with WV-2 images. They concluded that classifying the base object results in segmentation and classification, and has the best kappa coefficient, after which the neural network and the maximum likelihood classifier were ranked in the mean of accuracy.

In recent years, terrestrial laser scanner (TLS) has been used for forest inventory parameters assessment. Pazhouhan *et al.* [21] used of terrestrial laser scanner data in Hyricanian forest for extraction of individual tree parameters. The result showed the accurate measuring of trees height is difficult. The accuracy of diameter at breast height (DBH) by TLS is very suitable.

The aim of this study was to examine the potential of WV-2 satellite imagery for Zagros forest areas classification, using object-based image analysis (OBIA) and decision tree (DT) in the forests of surrounding Shiraz.

Materials and Methods

This experimental study was carried out in the Zagros mountain forests. The study comprised several operations applied to the preprocessed images that could be grouped into four main steps: Tree positioning by visual analysis; automatic detection of trees by Decision tree and object-based; identification of the best sets of parameters by an analysis of detection quality; validation with ground mapping.

The study area: The study area was part of the Haft Barm forest, which is located in Shiraz, Fars, Iran. The area contains different species of trees. This study considered forest mapping that significantly benefits the urban environment and temperature, thus resulting in high energy savings.

In this study, a radio-controlled four-propeller powered multicopter was used as a UAV remote sensing platform. The quadrocopter was a ready-made and commercially available Microdrones MD4-200 and is equipped with a GPS and Inertial Measurement Unit (IMU) for navigation and control.

Haft Barm lake set is located in the latitude from 51° 30" to 52° eastern and longitude from 29° 30' to 30° north in Fars province, Iran. These lakes are located 55Km west of Shiraz and northeast of the protected area of Arjan and Parishan. They are 2,150 meters above the sea level. The lakes have beautiful panoramic views of the hillocks and wetlands. The weather in this region is cold and dry in the winter and temperate in the summer. This area has an almost cold and semi-desert climate. Its catchment area is 16.9Km^2 and the average of annual precipitation is 1010mm [22]. Various plant species form the forest, pasture, and vegetation cover. Oak trees are the major forest species in the region that are densely covered by the area. Regarding the range of Arjan between the tropical region of southern Iran and the dry region of the south-east, the cold and semi-humid part of the northwest is an intermediate or ecotone region and it is very diverse in terms of plant species diversity.

This study was conducted on two different sites in the Haft-Barm area of Shiraz. The area of the first site (Baleh Zar village) is 106ha, and the second site of the Abe Anar village is 150ha (Figure 1).

A flowchart of work levels has been shown in figure 2.

The data that were used in this study included the image of the WorldView-2 satellite on May 21, 2015, with a resolution of 1.8m, and panchromatic bands (Spatial resolution of 0.5m) and UAV aerial imagery with a resolution of 3cm. Benchmark points were taken by three-frequency Global Positioning System (GPS) from the area.

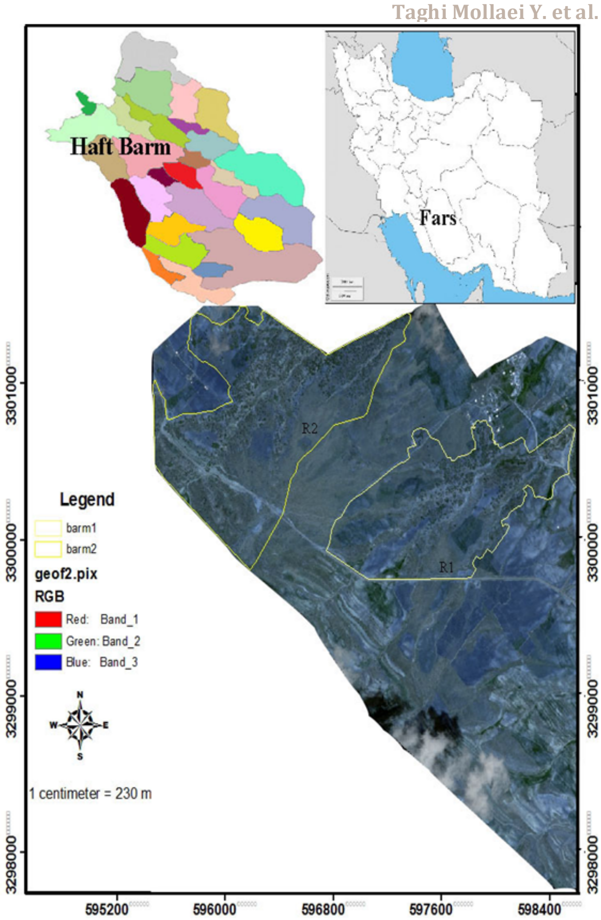

Figure 1) Location of Haft-Barm forest (WorldView-2 images captured on 21 May 2015); Yellow polygon is boundary of Region 1 (Baleh Zar) and region 2 (Abe Anar).

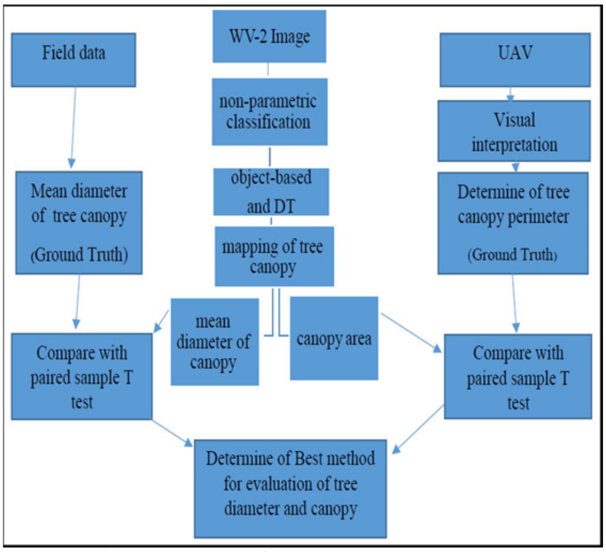

Figure 2) Flowchart of work levels

The Worldview-2 images were georeferenced, using the 9-point of three-frequency GPS, tracking real-time kinematic (RTK) and static ground reference; the Universal Transverse Mercator (UTM) coordinate system was considered, which was used to determine the points of the Benchmark points of the organization of mapping. Cloud computing points arrived from ArcGIS 10.4 and PCI Geomatica 16 software, and with accuracy, the average root means square error (RMSE) of 0.65 pixels was georeferenced, using the equation of degree three (ST order polynomia3). Then, Pansharpening images with a resolution of 0.5m were created with a combination of polygonal and panchromatic quadrants [23] (Table 1).

Table 1) Characteristics of sensor and four standard bands of WV-2

Wavelength (nm)	**Bands of WV-2 sensor**
450-800	panchromatic
450-510	blue
510-580	green
630-690	red
770-895	NIR1

In order to the inventory of trees perimeter in the forest area, pictures of drone images were taken by Phantom 4 Pro. Phantom 4 Pro is equipped with a one-inch CMOS (Complementary Metal-Oxide Semiconductor) camera that can capture 20-megapixel quality [24] (Figure 3). Weather conditions were sunny and calm with scattered cloud cover forming, during the time of image acquisition. Before each UAV flight, campaign was conducted 150 ground control points (GCPs; 50×50cm white panels) , were laid out in the field, and were logged with a high-precision differential global positioning system (DGPS; Leica GPS1200 Navigation Limited; Leica; German) for georeferencing purposes in order to support the image processing later on. Additionally, distinctive terrain objects (e.g., path, home, Nomad tent) were recorded.

Figure 3) The commercial "ready-to-use" Microdrones MD 4-200

The payload includes Inertial Measurement Unit (IMU), GPS receiver, downward pointing Colour Infrared (CIR)-modified digital Canon IXUS 100 camera, radio downlink, and microprocessor

Decision tree (DT): The first tree model was introduced to create a relationship between the independent and dependent variables [25]. The decision tree method has been used in previous studies for forestry [26, 27]. The decision tree is a classification process that repeatedly divides a series of educational data into smaller subsections based on experiments into one or more of the value of the complication [26, 28]. The decision tree has no similarity to most classifications, such as maximum likelihood (MLC), since it does not depend on the assumption [28]. In addition, unlike many other statistical analysis approaches, such as maximum likelihood classification, the decision tree does not depend on assumptions about value distribution or the independence of the variables from one another [29-31]. This is an advantage that we can integrate GIS data into a category that is often distributed widely and has many forms but it is highly correlated with one another [32, 26]. The Decision tree in ENVI/IDL is well implemented with remote sensing data and assigns each pixel to a particular class [26, 33, 34]. Due to the unique nature of oak trees in Zagros forests, their partitioning was based on the application of threshold values of spectral reflections, visual knowledge of data and user of the study area. Forest feature isolation was carried out, using the mean spectral value of the complication and determining the appropriate threshold in the 3 and 4th bands and the near infrared, as well as the index of the bonding ratio and the target cluster of vegetation (Equation 1):

$$R1 = \frac{R - NIR1}{R + NIR1} \quad (1)$$

R: red band, NIR: Near-Infrared 1 band

Nearest neighbor classifier

The classifier of nearest neighbor: Lists of nonparametric classifications of unknown pixels in accordance with the labels of the neighboring educational vectors in the image space [35] include as follow:

The best neighbor: Labels the nearest pixels surrounding the training pixel.

Nearest K: Assemblies are based on the majority of the training pixel tags near the neighbor k. The nearest neighbor k is the weighted distance. It assigns weights to the closest neighbor k, based on the label of the closest neighboring k instructional pixels, in the opposite proportion to the Euclidean distance of the unknown pixel, and assigns the label to the highest weight of the set.

In these methods, the distance between each unknown pixel and the training pixel must be calculated. If the spectrum of the classroom is massively and well-differentiated, the neighboring algorithm will produce similar results with the algorithm of the closest parametric mean.

Object-Based Classification: Pixel-based analysis is usually simple and operates in a comprehensive and general way on sensors. Although pixels are not often a favorite unit, it is not possible to measure without them. For example, the canopy of separate trees and gap between crowns involves several pixels and creates a spatial self-regulation within objects that we can easily detach in high-resolution images [36]. OBIA seems to search for a "mean" for objects; it searches objects by segmenting the image into groups of pixels with similar characteristics based on spatial and spatial properties [37].

The purpose of the image segmentation is to extract the image objects in the best case according to the scale features, the weight of the inhomogeneity of softness and the compression weight that was performed in the software. These parameters were obtained with estimation of scale parameter (ESP) and with test and error. Then, the objects obtained from this step enter the classification methods. Multi-resolution segmentation was done by the segmentation process. Using the approach of the nearest neighbor and identifying suitable training samples, the image was classified into two general forest and non-forest classes (Table 2).

Table 2) Weighting for segmentation

Factors	Hierarchy	
	Level 1	Level 2
Scale parameter	10	20
Color factor	0.8	0.8
Shape factor	0.2	0.2
Compactness degree	0.7	0.7
Softness degree	0.3	0.3

The most basic multi-resolution segmentation algorithm is the scale parameter. With determining the most accurate value of the scale parameter for image segmentation and it's verifying dealt several works in the past [38, 39]. For the purposes of this study in Zagros forest, Estimation of Scale Parameter (ESP) tool, which is used to estimate the scale parameter for multi-resolution segmentation in eCognition, was selected. ESP allows to select the default value of scale parameter, step size of scale parameter value incrementing, the number of repetitions, Shape and Compactness parameter values, on which iteratively performs segmentation of more-layered image at different levels of scale parameter, for which calculates the local variance of identified segments. If two pixels or the same object are merged, the rate of local variation will decrease, but if two pixels or non-sex objects are merged, the process of local variation changes will increase.

The graph represents the points where the ROC-LV, Local Variance (LV) and Rate of Change (ROC) suddenly increased when the pieces were merged and new larger parts were created, which is an appropriate scale for image segmentation. Based on the graphic evaluation of the LV and ROC calculations, which reflect the change of variance at different levels, it allows estimating the most appropriate scale parameter value for the image. The biggest changes in LV expressed by ROC values represent potentially the biggest changes in the meaning of segmentation and hence the representation of individual segments [39].

The best scales for the present image were 24, 26, 30, 34, 37, 31, 41, 45, 47, 49, 51, 54, 57, 60, 71, 75, 79, 88 and 94 (Diagram 1). Theoretically, the peaks in a ROC-LV curve indicate the levels where LV increases as segments delineate their correspondents in the real world.

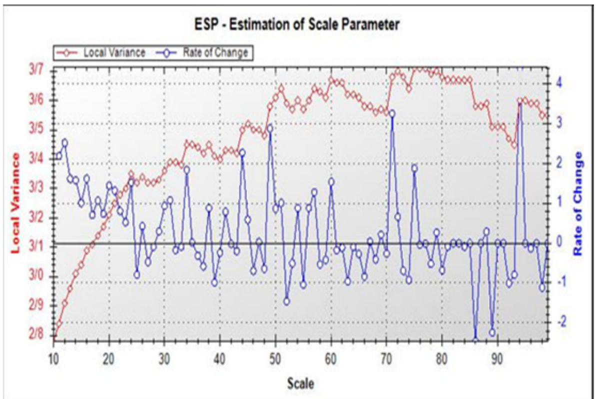

Diagram 1) Visualisation of rate of change in estimation of scale parameter (ESP) environment

After selecting the training data, they were arranged in a thematic layer, the training and test area (TTA) mask layer, in the software to be used during the process. The same training data was used for different classification methods. The classification was performed in three ways.

After extracting the forest feature in three methods, the results were validated. For this, 100 points were created randomly on the images, and the canopy boundary of these trees was determined from UAV images (Figure 4).

Figure 4) Canopy of 100 determined trees on UAV image for Ground truth

Accuracy assessment: Accuracy assessment was done in two ways; the first method was the usual method, which used the Kappa coefficient, and the second method was performed, using the Area under operating characteristic curve (AUC) method.

The sampling method for quantitative and qualitative forest characteristics: Sampling method of the present study was a systematic approach. A 200m×200m^2 grid was overlaid in the image of the region, with 40m×40m^2 sample plots marked into the area. A total of 63 sample plots (36 plots of Abe Anar village and 27 plots of Baleh Zar village) were measured at each site. In each plot, the characteristics of the vegetation considered included: The diameter of the large and small trees, the diameter at breast height (DBH), the tree crown cover, and the health of the tree were recorded.

Estimated canopy cover area for Baleh Zar forest trees on WV-2 and UAV images sampling with the 200×200m^2 network on the ground and satellite images of WV-2 was carried out. 27 plots of 1,600m^2 (40m×40m) were collected on site 1, the village of Baleh Zar and 33 plots in the site 2, the village of Abe Anar. In each sample piece, the large and small diameters, the diameter of the breasts and then the crown cover area (Formula 1) were measured.

The sample area was calculated on the basis of formula 1. Then, analysis of the canopy cover areas was carried out by SPSS 25 software.

Formula 1: Covering the crown surface=π/4×Medium crown diameter

The area of the canopy on the ground as an associated variable and canopy area on the satellite images were considered as an independent variable.

At first, the normal distribution of data was investigated by the Kolmogorov-Smirnov test. To compare the canopy coverage obtained from WV-2 satellite imagery and groundbreaking paired t-test was used at 95% confidence level. Multivariate regression analysis was used to predict quantitative variables in forest mapping. Also, the SPSS 25, Excel 2016, eCognation v. 8.7, ENVI 5, PCI Geomatica 16, and Google Earth 7.3 software were used.

Findings

There was no significant difference between the measurement of canopy coverage in UAV-DT and UAV-OBIA methods (Table 3; Diagrams 2 and 3).

Satellite imagery with an approximate magnitude of 0.95 (R^2=95%) illustrated the potential for high-resolution WV-2 satellite images (Tables 4 and 5).

Table 3) Comparison of the canopy coverage using two methods (UAV-DT and UAV-OBIA) in Baleh Zar and Abe Anar villages

Village name	Methods	Mean Difference	t-value	p-value
Baleh Zar				
Pair 1	UAV-DT	1.52±9.33	1.95	0.051
Pair 2	UAV-OBIA	1.78±9.02	1.97	0.058
Abe Anar				
Pair 1	UAV-DT	-3.98±21.01	-1.89	0.068
Pair 2	UAV-OBIA	-0.27±1.39	-1.94	0.071

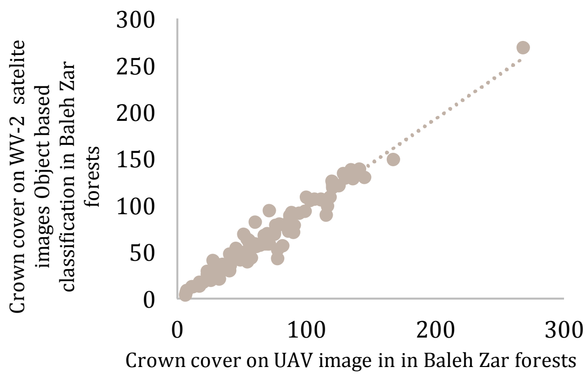

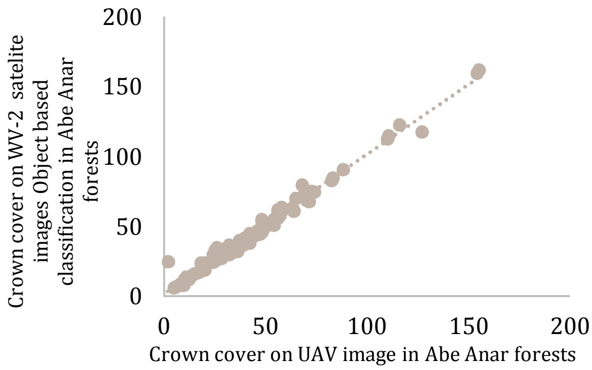

Diagram 2) Evaluation of the accuracy of the canopy in OBIA classification in satellite imagery wv-2 and UAV image in the forests of the village of Baleh Zar and Abe Anar (m^2)

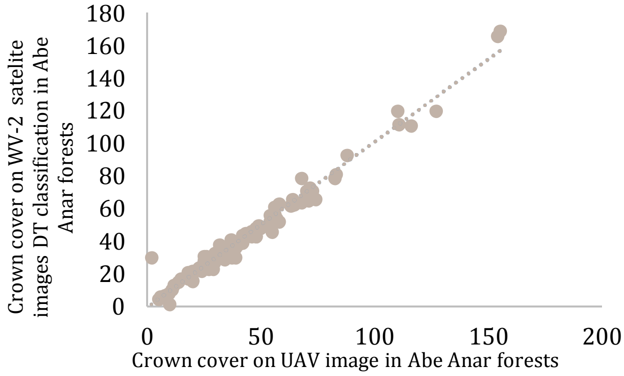

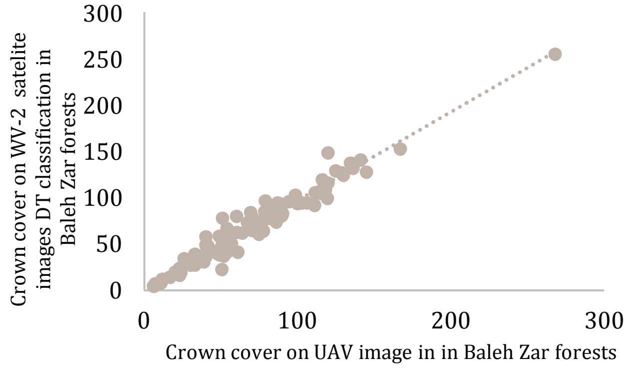

Diagram 3) Evaluation of the accuracy of the canopy in DT classification in satellite imagery WV-2 and UAV image in the forests of 2 sites (m^2)

Table 4) The mean of the canopy cover of trees (m^2) in the forests of Baleh Zar (n=100) and Abe Anar (n=100) villages

Village name	UAV	OBIA. WV-2 satellite images	DT. WV-2 satellite images
Baleh Zar	68.48±41.63	66.70±40.84	66.92±40.96
Abe Anar	44.62±28.9	44.89±28.68	44.23±30.11

Table 5) The statistical model of the canopy surface covering the satellite imagery of WV-2 and UAV of forests of two sites

Village name	Model	R^2	r	Statistical model
OBIA				
Baleh Zar	linear	0.953	0.976	Y=2.11+0.995X
Abe Anar	linear	0.998	0.999	Y=-0.579+1.007X
DT				
Baleh Zar	linear	0.964	0.982	Y=-0.893+0.943X
Abe Anar	linear	0.632	0.795	Y=12.314+0.665X

WV-2 satellite images can be used to estimate the canopy surface. The point cloud was plotted in diagrams 2 and 3 (In the X-axis, the crown surface on the satellite image and the Y-axis was the crown surface on the ground).

There was no significant difference between the measurement of canopy coverage in Dm Land-Dm DT and Dm Land-Dm OBIA methods (Table 6; Diagrams 4 and 5).

Satellite images with an approximate coefficient of 0.95 (R^2=95%) indicated that the average diameter of the canopy of trees can be obtained with high accuracy from satellite images of WV-2 (Tables 7 and 8).

Table 6) Comparison of the canopy coverage using two methods (Dm Land-Dm DT and Dm Land-Dm OBIA) in Baleh Zar and Abe Anar villages

Village name	Methods	Mean Difference	t-value	p-value (2tailed)
Abe Anar				
Pair 1	Dm Land-Dm DT	0.11±0.72	1.59	0.115
Pair 2	Dm Land-Dm OBIA	0.09±0.66	1.35	0.177
Baleh Zar				
Pair 1	Dm Land-Dm DT	0.16±1.01	1.60	0.113
Pair 2	Dm Land-Dm OBIA	0.14±0.99	1.50	0.136

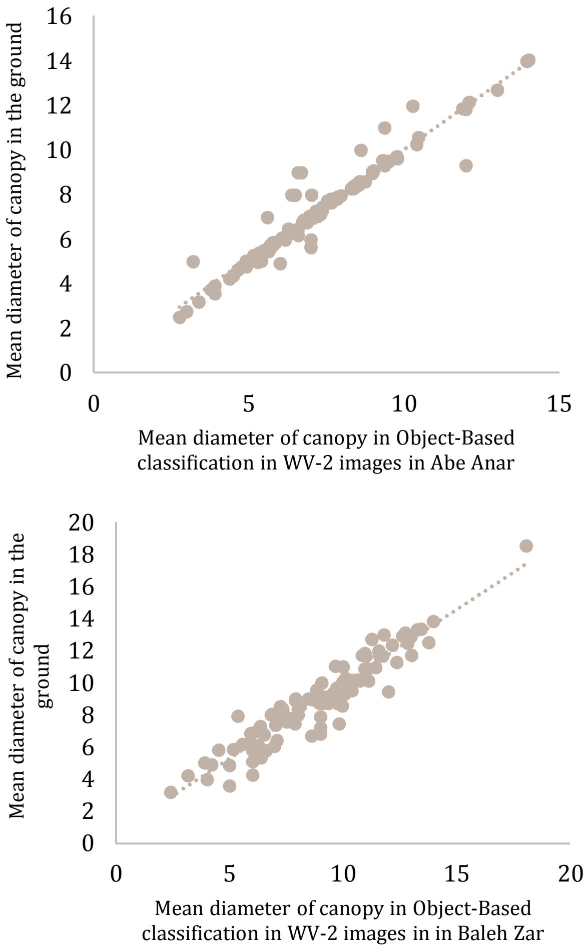

Diagram 4) Assessing the accuracy of the mean diameter of canopy in OBIA classification in WV-2 images and the ground of the trees in two sites (m^2)

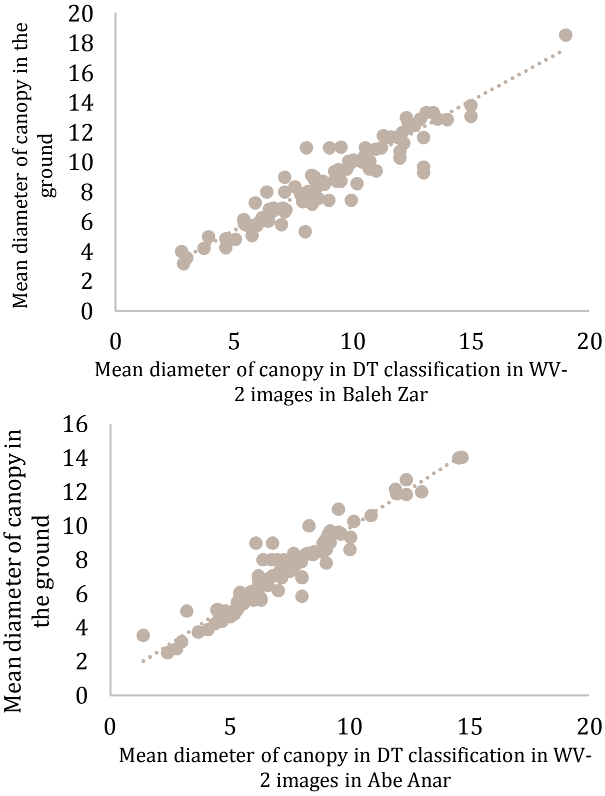

Diagram 5) Assessing the accuracy of mean diameter of canopy in DT classification in WV-2 images and on the ground of the trees in the forests of two sites (m^2)

Table 7) Statistical data of mean diameter of canopy of trees in Baleh Zar (n=100) and Abe Anar (n=100) forests

Sites	Mean±SD (m)
Baleh Zar	
Ground	9.13±2.96
OBIA	8.99±2.73
DT	8.97±2.78
Abe Anar	
Ground	7.37±2.32
OBIA	7.28±2.28
DT	7.25±2.43

Table 8) The statistical model of the mean diameter of canopy in WV-2 and ground of forests in two sites

Village name	Model	R^2	r	Statistical model
OBIA				
Baleh Zar	linear	0.942	0.888	Y=-0.028+1.020X
Abe Anar	linear	0.958	0.918	Y=0.256+0.976X
DT				
Baleh Zar	linear	0.828	0.963	Y=-0.035+0.991X
Abe Anar	linear	0.708	0.841	Y=1.372+0.790X

Satellite images with a good explanation coefficient of 0.68 (R^2=68%) indicated that height can be obtained with proper accuracy from satellite images of WV-2 (Table 9; Diagram 6 and 7).

Table 9) Statistical model of canopy surface in WV-2 images and tree height in the forests of two sites

Village name	model	R^2	r	Statistical model
OBIA				
Baleh Zar	linear	0.696	0.828	Y=5.117+0.056X
Abe Anar	linear	0.686	0.826	Y=4.112+0.069X
DT				
Baleh Zar	linear	0.683	0.827	Y=4.974+0.053X
Abe Anar	linear	0.600	0.775	Y=4.347+0.063X

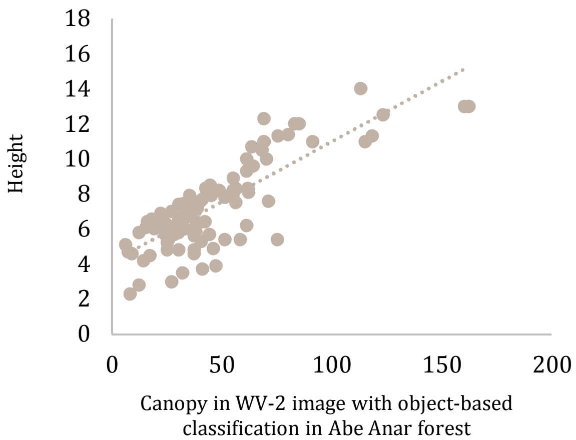

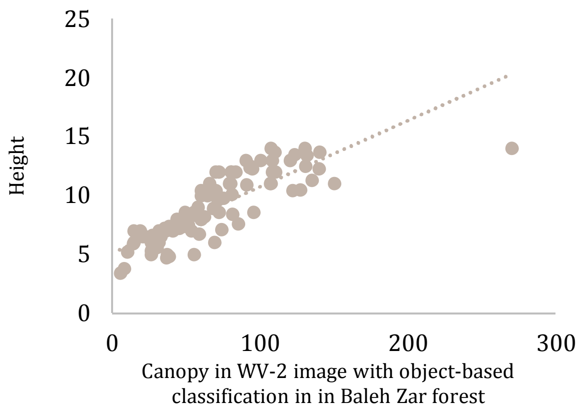

Diagram 6) Assessing the accuracy of the crown cover in OBIA classification in WV-2 images and the height of the trees in the forests of 2 sites (m^2)

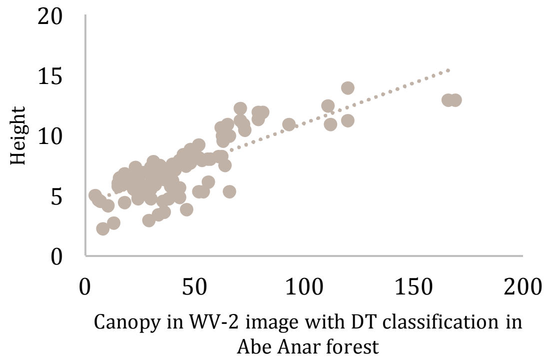

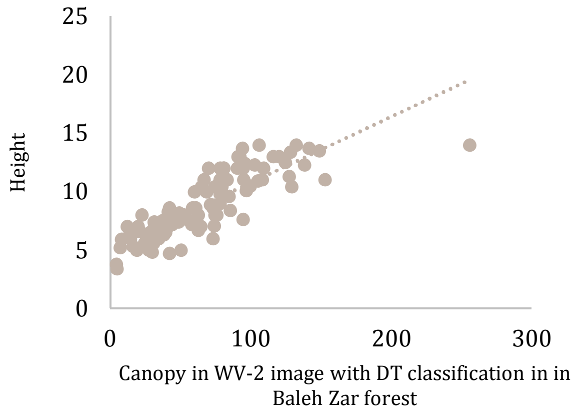

Diagram 7) Assessing the accuracy of the crown cover in DT classification in WV-2 images with the height of the trees in the forests of 2 sites

The validation of OBIA model using ROC curve revealed that the AUC of success and prediction rates were 0.98 and 0.93, respectively, which indicated the excellent capability of OBIA model in delineating forest area well potential in remote sensing (Table 10).
The quality of the classifications was almost the same. But there were differences in accuracy (Figure 5 and 6).

Table 10) Result of Receiver Operating Characteristic (ROC) in 2 sites

Indicators	Baleh Zar				Abe Anar			
	OBIA		DT		OBIA		DT	
	forest	other	forest	other	forest	other	forest	other
TP	4636	7654	7315	4358	2457	5543	4480	3289
FP	83	95	4	791	60	11	30	272
FN	95	83	791	4	11	60	272	30
TN	7654	4636	4358	7315	5543	2457	3289	4480
Specificity	0.989	0.982	0.373	0.902	0.989	0.995	0.991	0.943
Sensitivity	0.980	0.989	0.627	0.997	0.995	0.989	0.943	0.991
Precision	0.982	0.988	0.991	0.846	0.976	0.998	0.993	0.924
Accuracy	0.986	0.986	0.936	0.936	0.991	0.991	0.961	0.960
AUC	0.931	0.846	0.788	0.750	0.987	0.939	0.891	0.844

In this evaluation index, it was use the cells that are properly assigned to the target class (category) (TP), cells that are not properly assigned to the target class (TN), cells that are incorrectly assigned to the target class (FP) and cells that are not incorrectly assigned to the target class (FN).

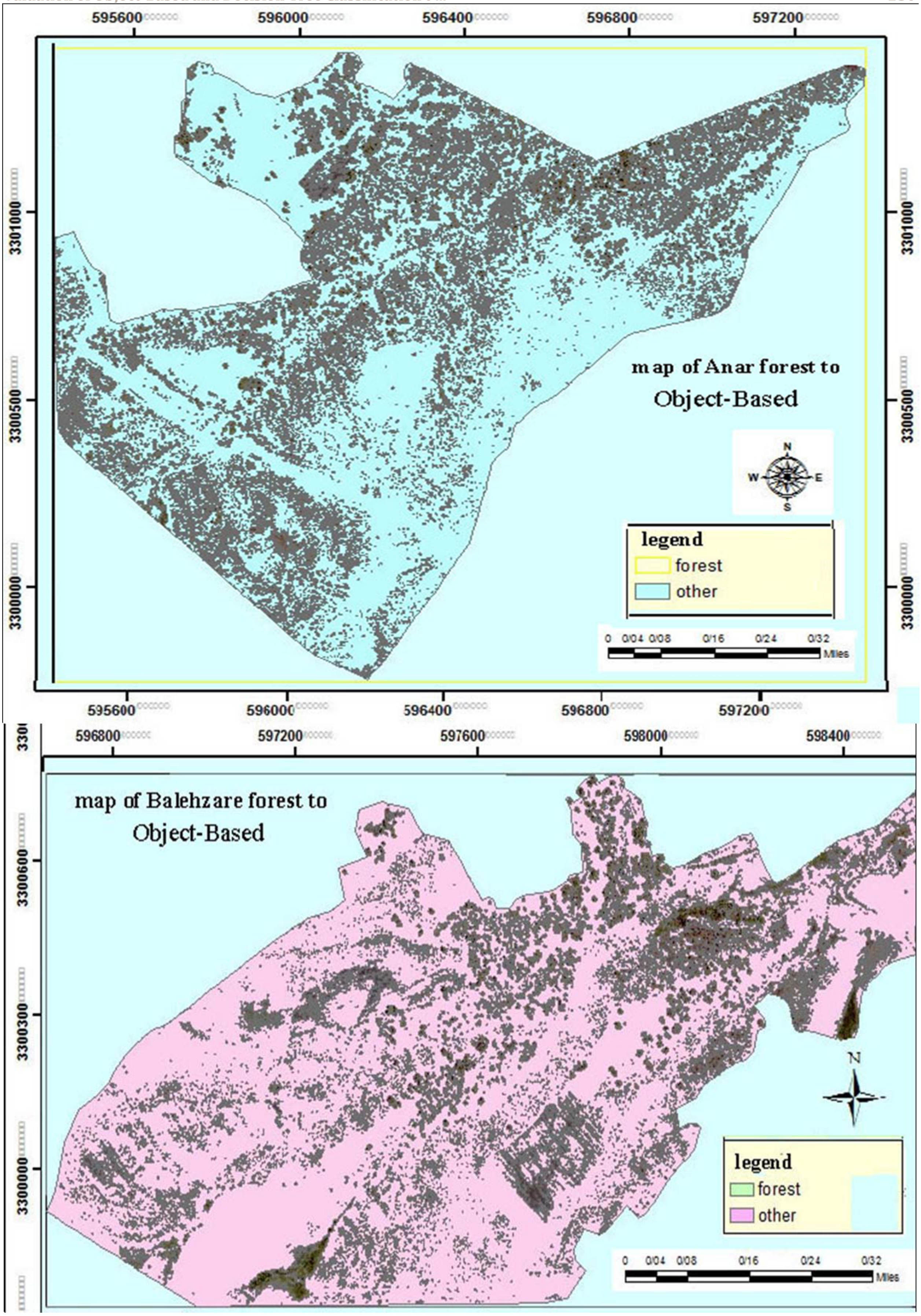

Figure 5) The results of the classification of forest feature with OBIA algorithm in Baleh Zare and Abe Anar sites

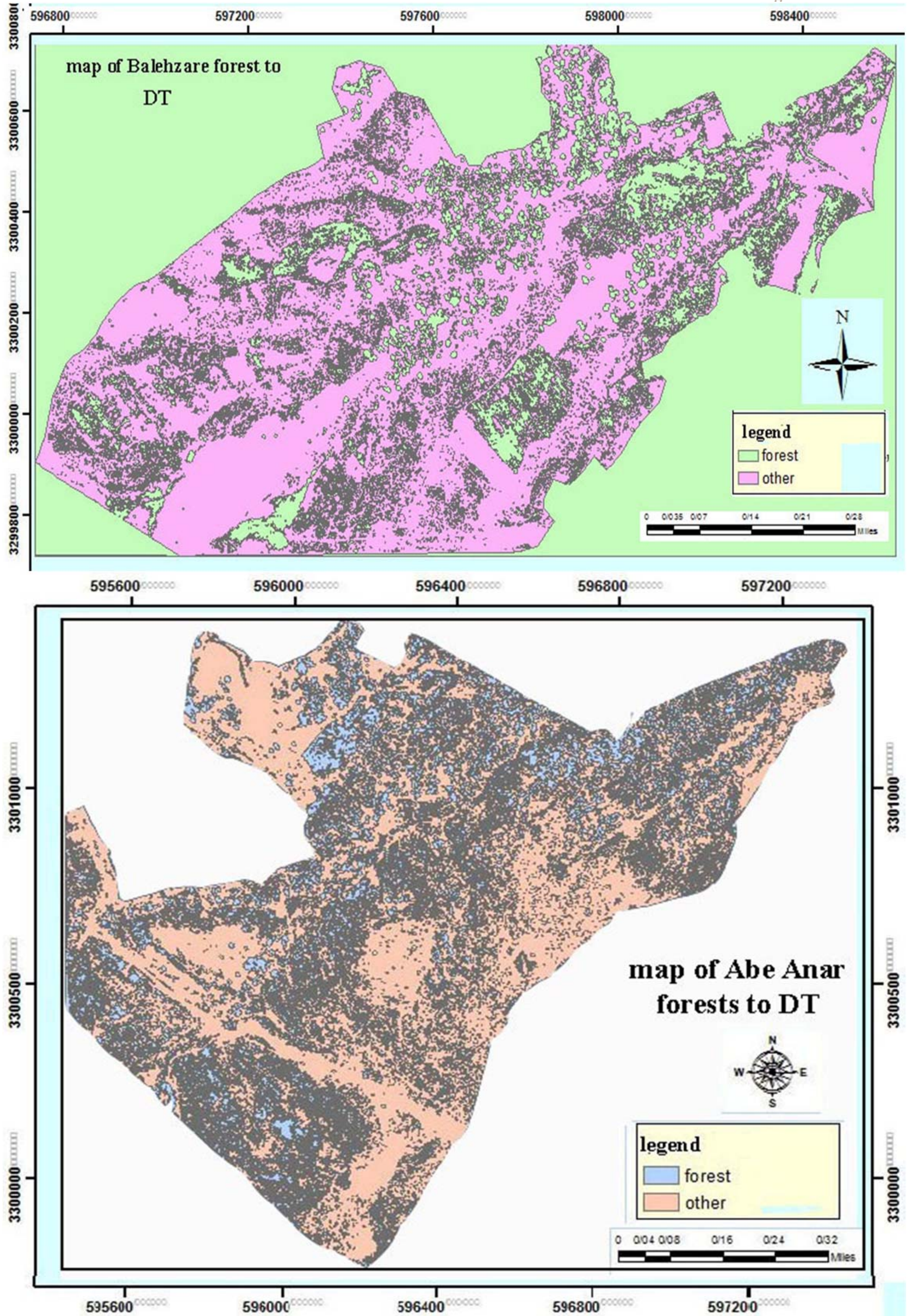

Figure 6) Map of forest feature with DT classification Baleh Zar village (site 1), Abe Anar village (site 2)

Table 11 summarizes the results of calculating the common indices in the decision tree and DT classification in the forests of two sites

Then the ROC (Receiver Operating Characteristic) curves were plotted (Diagram 8 and 9).

Table 11) Accuracy classification in two sites

Indexes/ class	**Abe Anar**		**Baleh Zar**	
	DT	OBIA	DT	OBIA
Prod Acc				
Forest	0.993	0.989	0.972	0.988
Class	0.941	0.996	0.921	0.978
User Acc				
Forest	0.920	0.998	0.929	0.987
Class	0.993	0.976	0.971	0.981
Kappa coefficient	0.924	0.981	0.898	0.967
Overall accuracy (%)	96.233	99.146	96.694	98.510

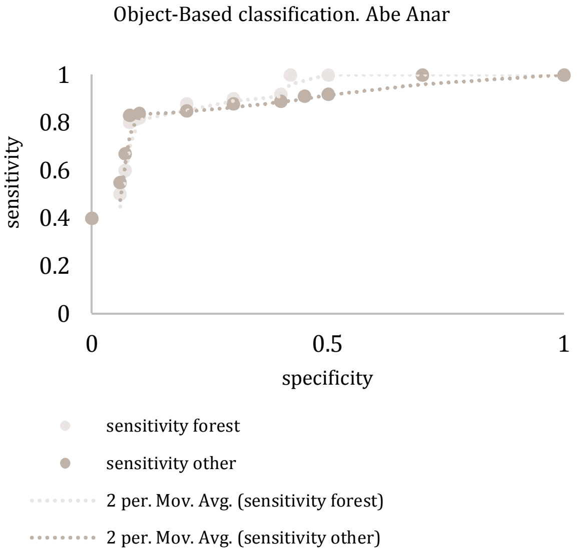

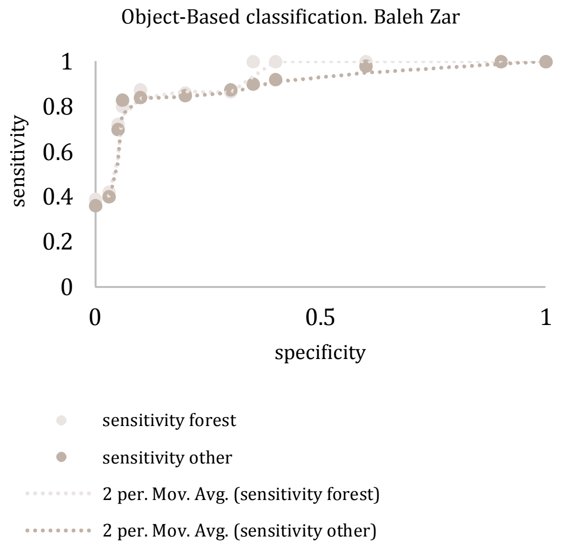

Diagram 8) ROC curve of OBIA classification in two sites

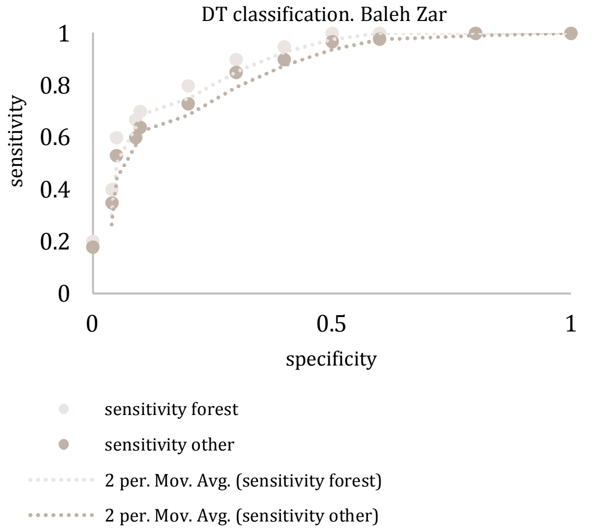

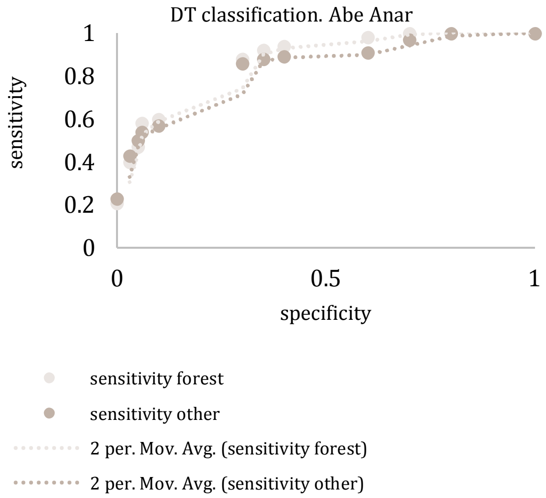

Diagram 9) ROC curve of DT classification in two sites

A high level of accuracy was obtained in estimating canopy cover, canopy diameter, and height of trees with satellite imagery. In the object-based method, the training samples were taken as TTA mask in order to evaluate the accuracy of the classification, using spectral data, and the Kappa coefficient was 0.974 (0.967 in the Abe Anar village and 0.981 in the village of Baleh Zar) and the overall accuracy of 98.82% (99.14% in the Abe Anar village and 98.51% in the Baleh Zar village) was obtained in the classification error matrix. Therefore, the base object method and decision tree method were respectively the highest classification accuracy in the study area (Table 12).

It was achieved an overall Kappa Index of Agreement (KIA) of 0.97 for Baleh Zar and 0.96 for Abe Anar site.

Table 12) Compare of OBIA classification in two sites with matrix

Classification accuracy	OBIA	DT
Kappa coefficient	0.974	0.908
Overall accuracy (%)	98.82	96.46

Training and Test Area MASK (TTA)

Discussion

The aim of this study was performance evaluation of the pixel-based classification (Decision tree method) and object-oriented classification methods, and using the WorldView-2 image of 2015 for oak trees mapping of forest regions of Haft-Barm Shiraz.

The present study focused on the suitability of single-date WorldView-2 data for forest mapping at the crown level in a Zagros forest test site located in Iran. For testing the sensor's potential in forest mapping, a large number of individual tree crowns from Oak tree species were manually delineated. The retrieved spectral signatures were analyzed with the Decision Tree (DE) and Object-Based classifier.

The WV-2 images can be used instead of land surveying to calculate the area of the canopy of forests, which is consistent with the results of the researchers. Forest mapping is the basic tools for administrators and land planners. Several methods have been proposed for trees mapping. The latest and most important methods are using remotely sensed data for forest mapping. This study is one of the first studies to estimate and extract single-tree parameters from high-resolution satellite imagery.

The results showed that the overall accuracy of all methods was 96%. This finding was consistent with the results of Wen *et al.* [40]. The findings of Wen *et al.* indicated that the method of classification of the base unit was placed in the first priority; next was the classification of the object, and base pixel for the Kappa coefficient was in the third stage. They concluded that the method of classification of piece base and object based on other methods in extracting urban trees in WV-2 images is superior.

Similarly, the findings of Immitzer *et al.,* [41] indicated that classifying objects instead of pixels the user's accuracies could be raised significantly for most tree species. The accuracy of Object-Based in this study was 92%.

Comparison of the land use area in the production map shows that the area of agricultural use, poor pasture, and residential land are almost in close proximity to the maps of the decision tree and the object-oriented algorithms.

OBIA is widely used for forest remote-sensing research [4, 42-44], and it has been very successful in forest tree studies [45-47].

In the present study, there was a good correlation between the diameters of the crown of trees with ground measurements measured with the drone, indicating that extracting from the data of the drone is excellent. So that the R coefficient for the crown diameter of the forest trees was averaged 0.85, which is consistent with the results of Shrestha and Wynne [48]. They also obtained a correlation coefficient of 0.9 for the crown diameter.

As Pande-Chhetri *et al.* [49] found in the estimation of wetland vegetation with WV-2 images, the object- based method was superior to the pixel-based method. In the current study, the object- based classification was also better than other classifications. The results of this study indicated that the object-based classification had a superior performance over the tree. It is suggested that object-oriented classification method be used to production of forest map in Zagros Mountain. The results of various land use classification methods show that the object-oriented method has an image with high resolution. The results obtained are Compatible with the studies of Thanh Noi [50], Raczko *et al.* [19], Pande-Chhetri *et al.* [49], Qian *et al.* [51], Shafri [52], Shao *et al.* [53], Amami *et al.* [54], Ghasemian *et al.* [55], Kim *et al.* [56].

Hao *et al.* [57] classified the Crop in North Xinjiang, China, with TM images, using Object-Based, SVM, maximum likelihood classier (MLC), neural network classier (NNC) and DT. The Object-Based was more accurate than SVM and DT in classification. In terms of algorithm stability, the Object-Based gave more stable overall accuracies than the other three algorithms except when trained, using 6% pixels with three variables. Of the other three algorithms, DT gave slightly more stable overall accuracies than ANN or the MLC, both of which gave overall accuracies in wide ranges.

The results of the present study, showed that the segmentation quality and the determination of segments had direct relation with the spatial resolution of the satellite image. By increasing the spatial resolution of the images and achieving a high resolution in the extraction of ground phenomena on the images, high-quality segments were produced and greatly increased the accuracy of the classification. This has been proven in other researches. This finding was consistent with the results of the studies of Hofmann *et al.*, [58], Chaudhuri and Sarkar [59], Baatz and Schäpe [60], Blaschke [61], Almeida *et al.* [62], Yan [63], Gao *et al.* [64], Zhaocong *et al.* [65], Platt and Schoennagel [66], Dehvari and Heck [67], Collingwood *et.al.* [68].

Segmentation accuracy for extraction of single tree crowns in UAV images is significantly related to the spatial resolution of images, but the internal parameters of the segmentation algorithm should also be appropriate and calibrated. This has been proven in Okojie's study [69].

Other factors such as the number of classes and the spatial and spatial accuracy of the sensors can also be affected to increase the accuracy. However, under the same conditions, accurate determination of the effective factors has a significant role in increasing accuracy. Therefore, the use of object-oriented and satellite images with spatial and spatial resolution is recommended in the satellite image classification process.

In the present study, there is no significant difference between ground data and satellite estimation. This indicates that the nonparametric models used in the study have no significant difference with ground reality. Considering other research on the extraction of the feature and using an algorithm, this study shows that the present study is of desirable accuracy.

Combining drone data with satellite data from WV-2 can be very useful for describing biodiversity and monitoring forest biodiversity

The very high correlation between the estimation of the canopy of the satellite images and terrestrial shows that canopy parameter can be estimated from the images. Although they are surveyed in trees in Zagros forests, forecast models of this study can be used for other forest levels with similar climates and similar species composition. This kind of forecast with drone images will help to properly assess the quality of carbon stored trees on the level of single trees.

Further studies should be developed to predict biophysical parameters such as leaf area index, stem volume and etc. Management tables for forest planners such as forestry activities, disaster vulnerability, and age class are useful for forest trees. The functionality of these models can improve inappropriate data from other forest levels, and if the area is not accessible, we can estimate trees from forest levels instead of being present in the field, using these equations. As the WorldView-2 satellite was launched only in 2009, studies employing this new sensor for vegetation analysis are still rare. Only little information about the benefits and limitations of the 8 spectral bands are available.

The high cost of purchasing satellite imagery, flying camera-equipped aircrafts and the three-frequency GPS were the limitations of this study.

It is suggested that in future studies, radar and optical data will be merged to enhance the quality of image processing.

Conclusion

Object-based classification results are better than the decision tree classification. WV-2 data can be used to predict tree parameters such as crown cover, bream diameter, tree height, tree number and biomass in the Zagros forests of Iran. The height of the trees can be obtained directly from the digital surface model with drone images. The crown cover and canopy diameter have a very high correlation with the terrestrial data. The object-based method in the extraction of single forest trees, using spectral data is more potent than pixel-based methods. WV-2 satellite spectral data in estimating the canopy surface are capable of estimating the quantitative characteristics of the crown cover of oak forests and extraction of single trees in the study area with proper accuracy.

Acknowledgments: We acknowledge the helpful comments of three anonymous reviewers.

Ethical permissions: The case was not found by the authors.

Conflicts of interests: The case was not found by the authors.

Authors' Contribution: Taghi Mollaei Y. (First author), Introduction author/ Original researcher (50%); Karamshahi A. (Second author), Methodologist/ Statistical analyst/ Discussion author (25%); Erfanifard S.Y. (Third author), Assistant researcher / Statistical analyst/ Discussion author (25%)

Funding/Support: This study was supported by the Shiraz University, Iran.

References

1- White JC, Stepper C, Tompalski P, Coops NC, Wulder MA. Comparing ALS and Image-Based Point Cloud Metrics and Modelled Forest Inventory Attributes in a Complex Coastal Forest Environment. For. 2015;6(10):3704-32.

2- Zöhrer F. Forstinventur: Ein leitfaden für studium und praxis. Hamburg: Parey; 1980. p. 207. [German]

3- Hudak AT, Haren, AT, Crookston NL, Liebermann RJ, Ohmann, JL. Imputing forest structure attributes from stand inventory and remotely sensed data in western Oregon, USA. For Sci. 2014;60(2):253-69.

4- Wulder MA, White JC, Hay GJ, Castilla G. Towards automated segmentation of forest inventory polygons on high spatial resolution satellite imagery. For Chron. 2008;84(2):221-30.

5- Allen CD, Macalady AK, Chenchouni H, Bachelet D, McDowell N, Vennetier M, et al. A global overview of drought and heat-induced tree mortality reveals emerging climate change risks for forests. For Ecol Manag. 2010;259(4):660-84.

6- Breshears DD, Cobb NS, Rich PM, Price KP, Allen CD, Balice RG, et al. Regional vegetation die-off in response to global-change-type drought. Proc Natl Acad Sci. 2005;102(42):15144-8.

7- Carnicer J, Coll M, Ninyerola M, Pons X, Sánchez G, Peñuelas J. Widespread crown condition decline, food web disruption, and amplified tree mortality with increased climate change-type drought. Proc Natl Acad Sci U S A. 2011;108(4):1474-8.

8- Phillips OL, Aragão LEOC, Lewis SL, Fisher JB, Lloyd J, López-González G, et al. Drought sensitivity of the Amazon rainforest. Science. 2009;323(5919):1344-7.

9- Van Mantgem PJ, Stephenson NL, Byrne JC, Daniels LD, Franklin J F, Fulé PZ, et al. Widespread increase of tree mortality rates in the western United States. Science. 2009;323(5913):521-4.

10. Karlson M, Reese H, Ostwald M. Tree crown mapping in managed woodlands (parklands) of semi-arid West Africa using WorldView-2 imagery and geographic object based image analysis. Sensors. 2014;14(12):22643-69.

11- Clark DB, Soto Castro C, Alvarado LDA, Read JM. Quantifying mortality of tropical rain forest trees using high spatial-resolution satellite data. Ecol Lett. 2004;7(1):52-9.

12- Clark DB, Read JM, Clark ML, Cruz AM, Dotti MF, Clark DA. Application of 1-M and 4-M resolution satellite data to ecological studies of tropical rain forests. Ecol Applications. 2004;14(1):61-74.

13- Gong P, Biging GS, Lee SM, Mei X, Sheng Y, Pu R, et al. Photo ecometrics for forest inventory. Geogr Inf Sci. 1999;5(1):9-14.

14- Leckie DG, Yuan X, Ostaff DP, Piene H, MacLean DA. Analysis of high spatial resolution multispectral MEIS imagery for spruce budworm damage assessment on a single tree basis. Remote Sens Environ. 1992;40(2):125-36.

15- Levesque J, J King D. Airborne digital camera image semivariance for evaluation of forest structural damage at an acid mine site. Remote Sens Environ. 1999;68(2):112-4.

16- Kelly M, Shaari D, Guo Q, Liu D. A comparison of standard and hybrid classifier methods for mapping hardwood mortality in areas affected by “sudden oak death”. Photogramm Eng Remote Sens. 2004;70:1229-39.

17- Sedliak M, Sačkov I, Kulla L. Classification of tree species composition using a combination of multispectral imagery and airborne laser scanning data. Cent Eur For J. 2017;63(1):1-9.

18- Niphadkar M, Nagendra H, Tarantino C, Adamo M, Blonda P. Comparing pixel and object-based approaches to map an understory invasive shrub in tropical mixed forests. Front Plant Sci. 2017;8:892.

19- Raczko E, Zagajewski B. Comparison of support vector machine, random forest and neural network classifiers for tree species classification on airborne hyperspectral APEX images. Eur J Remote Sens. 2016;50(1):144-54.

20- Juniati E, Arrofiqoh EN. Comparison of Pixel-Based and Object-Based classification using parameters and non-parameters approach for the pattern consistency of multi scale landcover. Int Arch Photogramm Remote Sens Spatial Inf Sci. 2017;XLII-2/W7:765-71.

21- Pazhouhan I, Najafi A, Kamkar Rouhani A, Vahidi J. Extraction of individual tree parameters by using terrestrial laser scanner data in Hercynian forest. Ecopersia. 2017;5(3):1837-47.

22- Alem H, Mohammadi Z. Determining the water sources of lakes: A case study of lakes Haftbarm, Fars Province, Iran. Int Bull Water Resour Develop. 2014;2(2 suppl 5). [Persian]

23- Updike T, Comp C. Radiometric use of worldview-2 imagery [Internet]. Westminster: Digital Globe; 2010 [cited 2015 May 22]. Available from: https://www.yumpu.com/en/document/view/43552535/radiometric-use-of-worldview-2-imagery-technical-note-pancroma

24- DJI. PHANTOM 4 user manual [Internet]. Shenzhen: DJI; 2016 [cited 2018 March 11]. Available from: https://dl.djicdn.com/downloads/phantom_4/en/Phantom_4_User_Manual_en_v1.0.pdf.

25- Quinlan JR . Learning with continuous classes. World Sci. 1992:343-8.

26- Liang S, Liu J, Liang M. Ecological study on the mangrove communities in Beilunhekou national nature reserve. J Guangxi Norm Univ Natl Sci Ed. 2004;22(2):70-6 [Chinese]

27- Heumann BW. An Object-Based classification of mangroves using a hybrid decision tree—support vector machine approach. Remote Sens. 2011;3(11):2440-60.

28- Tooke TR, Coops NC, Goodwin NR, Voogt JA. Extracting urban vegetation characteristics using spectral mixture analysis and decision tree classifications. Remote Sens Environ. 2009;113(2):398-407.

29. Ghose MK, Pradhan R, Sushan Ghose S. Decision Tree Classification of Remotely Sensed Satellite Data using Spectral Separability Matrix. Int J Adv Comput Sci Appl. 2010;1(5):93-101

30- Friedl MA, Brodley CE. Decision tree classification of land cover from remotely sensed data. Remote Sens. Environ. 1997;61(3):399-409.

31- Pal M, Mather PM. An assessment of the effectiveness of decision tree methods for land cover classification. Remote Sens Environ. 2003;86(4):554-65.

32- Jensen JR. Introductory digital image processing: A remote sensing perspective. 3rd Edition. Upper Saddle River: Prentice Hall; 2005.

33- Quinlan JR. Induction of decision trees. Mach Learn. 1986;1(1):81-106.

34- Xu M, Watanachaturaporn P, Varshney PK, Arora MK.

Decision tree regression for soft classification of remote sensing data. Remote Sens Environ. 2005;97(3):322-36.
35- Schowengerdt RA. Remote Sensing: Models and methods for image processing. Cambridge: Academic press; 1997.
36- Woodcock CE, Strahler AH. The factor of scale in remote sensing. Remote Sens Environ. 1987;21(3):311-32.
37- Benz UC, Hofmann P, Willhauck G, Lingenfelder I, Heynen M. Multi-resolution, object-oriented fuzzy analysis of remote sensing data for GIS-ready information. ISPRS J Photogramm Remote Sens. 2004;58(3-4):239-58.
38- Drăguţ L, Tiede D, Levick SR. ESP: A tool to estimate scale parameter for multiresolution image segmentation of remotely sensed data. Int J Geogr Inf Sci. 2010;24(6):859-71.
39- Drăguţ L, Csillik O, Eisank C, Tiede D. Automated parameterisation for multi-scale image segmentation on multiple layers. ISPRS J Photogramm Remote Sens. 2014;88:119-27.
40- Wen D, Huang X, Liu H, Liao W, Zhang L. Semantic classification of urban trees using very high resolution satellite imagery. IEEE J Sel Top Appl Earth Observ Remote Sens. 2017;10(4):1413-24.
41. Immitzer M, Atzberger, Koukal T. Tree Species Classification with Random Forest Using Very High Spatial Resolution 8-Band WorldView-2 Satellite Data. Remote Sens. 2012;4(9):2661-93.
42- Chubey MS, Franklin SE, Wulder MA. Object-based analysis of Ikonos-2 imagery for extraction of forest inventory parameters. J Am Soc Photogramm Remote Sens. 2006;72(4):383-94.
43- Desclée B, Bogaert P, Defourny P. Forest change detection by statistical object-based method. Remote Sens Environ. 2006;102(1-2):1-11.
44- Hay GJ, Castilla G, Wulder MA, Ruiz JR. An automated object-based approach for the multiscale image segmentation of forest scenes. Int J Appl Earth Observ Geoinf. 2005;7(4):339-59.
45- Zhang Zh, Kazakova A, Moskal LM, Styers DM. Object-Based Tree Species Classification in Urban Ecosystems Using LiDAR and Hyperspectral Data. For. 2016;7(6):122
46- Myint SW, Giri CP, Wang L, Zhu Z, Gillette SC. Identifying mangrove species and their surrounding land use and land cover classes using an object-oriented approach with a lacunarity spatial measure. J GIScience Remote Sens. 2008;45(2):188-208.
47- Wang L, Sousa WP, Gong P. Integration of object-based and pixel-based classification for mapping mangroves with IKONOS imagery. Int J Remote Sens. 2004;25(24):5655-68.
48- Shrestha R, Wynne RH. Estimating biophysical parameters of individual trees in an urban environment using small footprint discrete-return imaging Lidar. Remote Sens. 2012;4(2):484-508.
49- Pande-Chhetri R, Abd-Elrahman A, Liu T, Morton J, Wilhelm VL. Object-based classification of wetland vegetation using very high-resolution unmanned air system imagery. Eur J Remote Sens. 2017;50(1):564-76.
50- Thanh Noi P, Kappas M. Comparison of random forest, k-nearest neighbor, and support vector machine classifiers for land cover classification using Sentinel-2 imagery. Sensors. 2017;18(1).
51- Qian Y, Zhou W, Yan J, Li W, Han L. Comparing machine learning classifiers for Object-Based land cover classification using very-high-resolution imagery. Remote Sens. 2015;7(1):153-68.
52- Shafri HZM, Ramle FSH. A comparison of support vector machine and decision tree classifications using satellite data of Langkawi island. Inf Technol J. 2009;8(1):64-70.
53- Shao Y, Lunetta RS. Comparison of support vector machine, neural network, and CART algorithms for the land-cover classification using limited training data points. ISPRS J Photogramm Remote Sens. 2012;70:78-87.
54- Amami R, Ben Ayed D, Ellouze N. An Empirical comparison of SVM and some supervised learning algorithms for vowel recognition. Int J Intell Inf Proc. 2012;3(1).
55- Ghasemian N, Akhondzadeh M. Comparison of methods of artificial neural networks, support vector machine and decision tree to identify clouds in Landsat 8 satellite images. Geospat Eng J. 2016;7(4):25-36. [Persian]
56- Kim J, Kim BS, Savarese S. Comparing image classification methods: K-nearest-neighbor and support-vector-machines. AMERICAN-MATH'12/CEA'12 Proceedings of the 6th WSEAS international conference on computer engineering and applications, and proceedings of the 2012 American conference on applied mathematics. Stevens Point: World Scientific and Engineering Academy and Society (WSEAS); 2012.
57- Hao P, Wang L, Niu Z. Comparison of hybrid classifiers for crop classification using normalized difference vegetation index time series: A case study for major crops in North Xinjiang, China. PLoS One. 2015;10(9):e0137748.
58- Hofmann T, Puzicha J, Buhmann JM. Unsupervised texture segmentation in a deterministic annealing framework. IEEE Transactions Pattern Anal Mach Intell. 1998;20(8):803-18.
59- Chaudhuri BB, Sarkar N. Texture segmentation using fractal dimension. IEEE Transactions Pattern Anal Mach Intell. 1995;17(1):72-7.
60- Baatz M, Schäpe A. Multiresolution segmentation-an optimization approach for high quality multi-scale image segmentation. In: Strobl J, editor. Angewandte geographische informationsverarbeitung XII: Beiträge zum AGIT- symposium Salzburg. Karlsruhe: Wichmann Verlag; 2000. pp. 12-23. [German]
61- Blaschke T. Object-based image analysis for remote sensing. ISPRS J Photogramm Remote Sens. 2010;65(1):2-16.
62- Almeida CM, Souza IM, Durand Alves C, Pinho CMD, Pereira MN, Feitosa RQ. Multilevel object-oriented classification of quick bird images for urban population estimates. GIS '07 Proceedings of the 15th annual ACM international symposium on advances in geographic information systems, Seattle, WA, USA — November 07 - 09, 2007. New York: ACM; 2007.pp. 5.
63- Yan G. Pixel-based and object-oriented image for coal fire research [Internet]. City publisher: publisher; 2003 [cited 2015 May 18]. Available from: http://www.ecognition.com/sites/default/files/gao_yan.pdf.
64- Gao Y, Mas JF, Navarrete A. The improvement of an object-oriented classification using multi-temporal MODIS EVI satellite data. Int J Digit Earth. 2009;2(3):219-36.
65- Zhaocong W, Lina Y, Maoyun Q. Granular approach to object-oriented remote sensing image classification. In: Wen P, Li Y, Polkowski L, Yao Y, Tsumoto S, Wang G, editors. International conference on rough sets and knowledge technology. Heidelberg: Springer; 2009. pp. 563-70.

66- Platt RV, Schoennagel T. An object-oriented approach to assessing changes in tree cover in the Colorado Front Range 1938-1999. For Ecol Manag. 2009;258(7):1342-9.
67- Dehvari A, Heck RJ. Comparison of object-based and pixel-based infrared airborne image classification methods using DEM thematic layer. J Geogr Reg Plan. 2009;2(4):086-96.
68- Collingwood A, Steven EF, Guo X, Stenhouse G. A medium-resolution remote sensing classification of agriculture areas in Alberta grizzly bear habit. Can J Remote Sens. 2009;35(1):22-36.
69- Okojie J. Assessment of forest tree structural parameter extractability from optical imaging UAV dataset [Dissertation]. Enschede: University of Twente; 2017.